

University of Nebraska - Lincoln

DigitalCommons@University of Nebraska - Lincoln

David Sellmyer Publications

Research Papers in Physics and Astronomy

2012

Aligned and exchange-coupled L10 (Fe,Co)Pt-based magnetic films

Yi Liu

University of Nebraska-Lincoln, yliu@unl.edu

Thomas A. George

University of Nebraska - Lincoln, tgeorge1@unl.edu

Ralph Skomski

University of Nebraska-Lincoln, rskomski2@unl.edu

David J. Sellmyer

University of Nebraska-Lincoln, dsellmyer@unl.edu

Follow this and additional works at: <https://digitalcommons.unl.edu/physicsellmyer>



Part of the [Physics Commons](#)

Liu, Yi; George, Thomas A.; Skomski, Ralph; and Sellmyer, David J., "Aligned and exchange-coupled L10 (Fe,Co)Pt-based magnetic films" (2012). *David Sellmyer Publications*. 234.

<https://digitalcommons.unl.edu/physicsellmyer/234>

This Article is brought to you for free and open access by the Research Papers in Physics and Astronomy at DigitalCommons@University of Nebraska - Lincoln. It has been accepted for inclusion in David Sellmyer Publications by an authorized administrator of DigitalCommons@University of Nebraska - Lincoln.

Aligned and exchange-coupled $L1_0$ (Fe,Co)Pt-based magnetic films

Y. Liu,^{a)} T. A. George, R. Skomski, and D. J. Sellmyer

Department of Physics and Astronomy and Nebraska Center for Materials and Nanoscience, University of Nebraska, Lincoln, Nebraska 68588, USA

(Presented 31 October 2011; received 23 September 2011; accepted 3 December 2011; published online 12 March 2012)

Films of aligned $L1_0$ -structure (Fe,Co)Pt with *fcc* Fe(Co,Pt) are synthesized by co-sputtering Fe, Co, and Pt on an (001) MgO substrate with *in situ* heating at 830 °C. The nanostructures and magnetic properties of the films are characterized by X-ray diffraction (XRD), transmission electron microscopy (TEM), and superconducting quantum interference device (SQUID). The compositions of the samples $(\text{Fe,Co})_x\text{Pt}_{1-x}$ are designed to maintain an atomic Fe: Co ratio of 65:35 while increasing the Fe,Co content in each successive sample. In samples with low Fe and Co concentration, the XRD patterns exhibit three strong peaks, namely $L1_0$ (Fe,Co)Pt (001), $L1_0$ (Fe,Co)Pt (002), and MgO (002). A fourth peak is observed in samples with high Fe and Co concentration and identified as *fcc* (002). The XRD patterns confirm the formation of $L1_0$ -ordered (Fe,Co)Pt and its epitaxial growth on MgO. TEM shows that the (Fe,Co)Pt films form isolated magnetic grains of about 100 nm in diameter. Hysteresis-loop measurements show that the increase of the Fe,Co concentration from 57.3 to 68.3 at % enhances the saturation magnetization M_s from 1245 emu/cm³ to 1416 emu/cm³, and the coercivity decreases from 32 kOe to 8.9 kOe. The nominal maximum energy product per grain is 64 MGOe. © 2012 American Institute of Physics. [doi:10.1063/1.3679099]

I. INTRODUCTION

A key figure of merit of permanent magnets is the energy product $(BH)_{\text{max}}$. The achievable maximum energy product is determined by its saturation magnetization M_s and its magnetic anisotropy, $(BH)_{\text{max}} \leq 4\pi^2 M_s^2$. In the past, the achievement of energy product record has been a result of discovery of new compounds with high magnetization and high anisotropy. However, the discovery of new compounds with better magnetic properties than Nd₂Fe₁₄B has proven to be difficult. Another approach to increase the energy product is to exchange-couple an existing hard-magnetic compound to a soft phase with high M_s .¹⁻³ Various attempts have been made to synthesize exchange-coupled magnets.⁴⁻⁶ To maximize the energy product of exchange-coupled magnets, it is important to ensure high magnetization of the soft and the hard phases while maintaining the anisotropy and crystallographic alignment of the hard phase. We have recently shown⁶ that $L1_0$ FePt + *fcc* Fe(Pt) hard and soft phase nanostructure exchange coupled magnet has excellent magnetic properties and high nominal energy product up to 54 MGOe. The easy axis of the hard phase $L1_0$ FePt is aligned by using the (001) MgO single crystal. To increase the energy product further, we considered the choice of both hard phase and soft phase. Fe₆₅Co₃₅ has the highest M_s of 1950 emu/cm³ known so far. It is therefore the most suitable soft phase for M_s enhancement. In consideration of phase equilibrium with the soft phase, $L1_0$ (Fe,Co)Pt is a good choice if it is stable and can coexist with Fe₆₅Co₃₅. Maclaren *et al.* performed first-principles calculations of the electronic structure of $L1_0$ (FeCo)Pt.⁷ They found that the Fe and Co moments are both

slightly enhanced over respective bulk values and show behaviors typical of the atoms at interfaces where the number of like coordinating atoms is reduced. The system shows phase separation below 650°C above which a continuous $L1_0$ structure of (Fe,Co)Pt is formed. If the stable $L1_0$ structure of (Fe,Co)Pt is formed in which Fe atoms have more neighbors of Co atoms and vice versa, enhanced Fe moment can be expected. In this paper we report our experimental investigation of phase formation and magnetic properties of various Fe-Co-Pt films containing magnetic hard and soft phases. Our goal is to synthesize and investigate the potential for nanostructured exchange-coupled magnets with higher energy products. Because Fe₆₅Co₃₅ is known to have the highest magnetization, the Fe: Co atomic ratio is chosen to be 65: 35 for all samples in this work.

II. EXPERIMENTAL PROCEDURE

An AJA International sputtering system was used for film deposition. (Fe,Co)Pt films were deposited on (001) oriented single-crystal MgO by sputtering Fe, Co, and Pt targets. The sputtering rates of Fe, Co, and Pt were adjusted to deposit films with various Fe, Co, and Pt concentrations. The compositions were calculated using the sputtering rates of Fe, Co, and Pt, which were determined by X-ray reflectivity measurements of the film thicknesses. Each time before deposition, a vacuum of better than 4×10^{-8} Torr was achieved in the deposition chamber, and the Ar pressure for deposition was 5 mTorr. The films were characterized using a Rigaku x-ray diffractometer and a JEOL 2010 transmission electron microscope (TEM). The magnetic properties were measured in a Quantum Design SQUID magnetometer up to a maximum applied field of 70 kOe at room temperature.

^{a)}Electronic mail: yliu1@unlserve.unl.edu.

III. RESULTS

First we used X-ray diffraction (XRD) to confirm the formation of $L1_0$ -ordered (Fe,Co)Pt and its epitaxial growth on MgO(001). Figure 1 shows the XRD patterns for three samples with different atomic concentrations of Fe,Co: 57.3%, 61.8%, and 62.9%. In the first two samples, only three peaks are observed. The MgO (002) peak is the strongest peak due to the large volume of the MgO substrate. Two (Fe,Co)Pt peaks, namely (001) and (002), are identified in perfect agreement with the calculated solid lines for the $L1_0$ structure (bottom part of Fig. 1). The fcc (002) peak in the sample with 62.9 at% Fe,Co is identified by calculation (dotted line) and corresponds to lattice parameter of $a = 3.797$ Å. The dashed line is the (001) diffraction intensity from the $L1_2$ structure (Fe,Co)₃Pt if it is formed. The absence of a corresponding peak in the experiment indicates that no $L1_2$ ordering occurs. Therefore, this fcc phase has Fe as the majority element, with Co and Pt entering the Fe lattice randomly. The Co and Pt atoms stabilize the fcc phase. The fcc structure phase is magnetically soft but has high magnetization. Interestingly, the (111) peak, which is the strongest peak in randomly oriented fcc and $L1_0$ samples, is not observed. This indicates that both the $L1_0$ -phase and fcc phase grow epitaxially on the MgO substrate.

Figure 2 shows that the (Fe,Co)Pt films grow on the MgO substrate in the form of separated islands. Each island is a magnetic grain which is a mixture of both hard and soft magnetic phases. In the present case, the magnetic hard phase is identified as the $L1_0$ (FeCo)Pt and magnetic soft phase fcc Fe(Co,Pt). Due to their high mobility at 830 °C, the atoms form small individual magnetic grains that grow as the deposition process continues and reach an average size of about 100 nm. Since these magnetic grains do not form a continuous film, they must remain supported by the MgO layer during the TEM investigation. The MgO blurs the contrast between the $L1_0$ and fcc phases. However, the

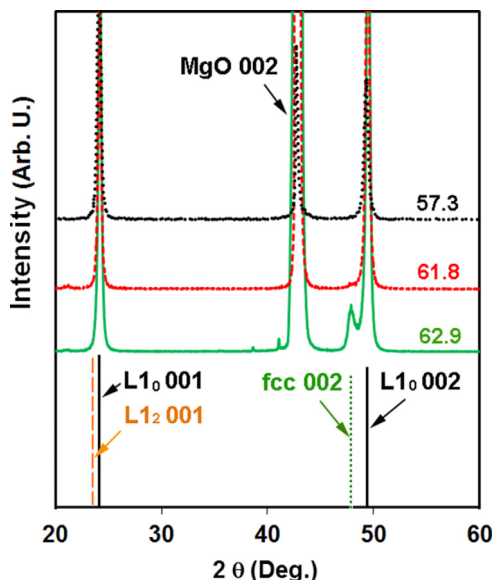


FIG. 1. (Color online) X-ray diffraction patterns of FeCoPt films on MgO. The Fe,Co content (at %) of each sample is shown in the figure.

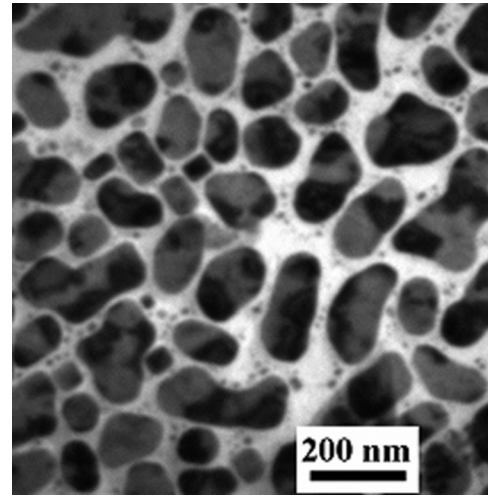


FIG. 2. TEM image of the FeCoPt film with 61.8 at% Fe,Co. The contrast of the background is from the MgO substrate.

gaps between the magnetic grains improve the coercivity by magnetically decoupling them.

The superconducting quantum interference device (SQUID) measurements were performed at room temperature in magnetic fields applied in-plane (\parallel) and perpendicular to the film plane (\perp). The loops of the thin films are affected by internal demagnetizing field. Here we used the method of estimating the internal field by setting $dM/dH = \infty$ at $H = H_c$.⁸ This correction does not change the M_s and H_c . But it does change the energy product. Figure 3 shows the hysteresis loops of (Fe,Co)Pt based films with the correction

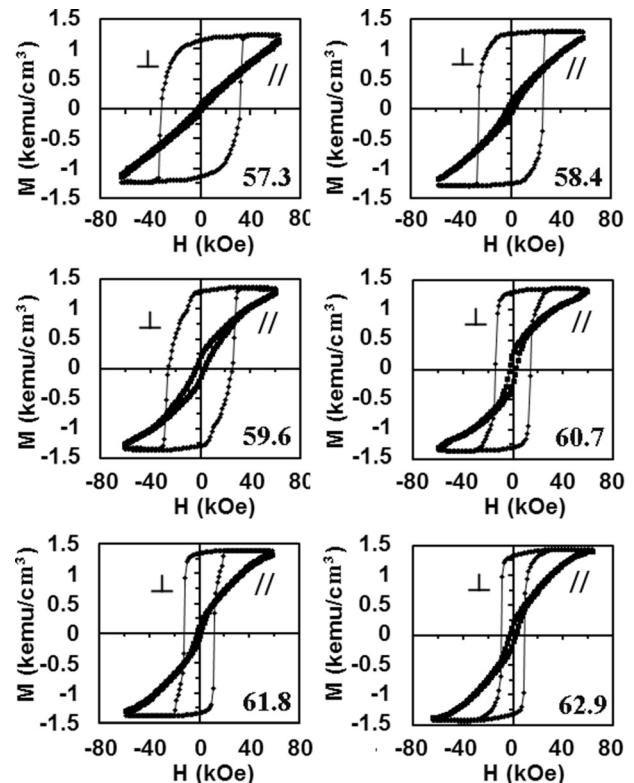


FIG. 3. In-plane (\parallel) and out-of-plane (\perp) hysteresis loops of FeCoPt films. The figures are labeled by the Fe,Co content of the samples in at%.

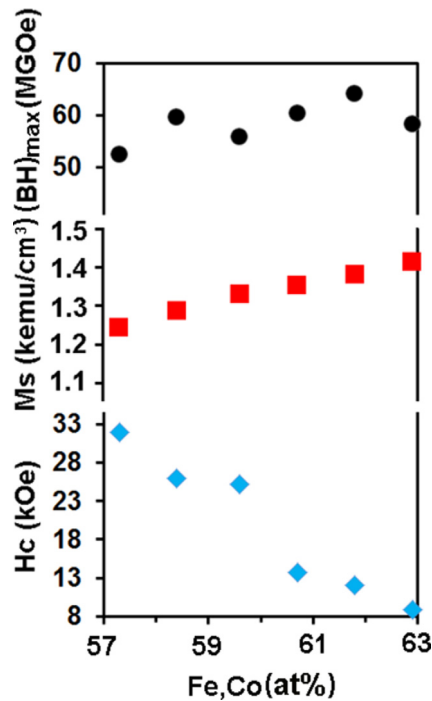


FIG. 4. (Color online) Coercivity H_c , saturation magnetization M_s , and nominal energy product as functions of Pt concentration.

discussed above. As expected for aligned magnets, there is a significant difference between the out-of-plane loops and in-plane loops. The coercivity H_c , saturated magnetization M_s and energy product $(BH)_{max}$ for (\perp) loops are plotted in Fig. 4. The coercivity H_c decreases while M_s increases with increasing Fe,Co content. The nominal energy product $(BH)_{max}$ reaches 64 MGOe at the sample with 61.8 at% Fe,Co. The measured magnetic properties are listed in Table I.

IV. DISCUSSION

The XRD pattern of the sample with 62.9 at% Fe,Co reveals the existence of a soft-magnetic *fcc* phase. By contrast, the sample with 57.3 at% Fe,Co does not contain this *fcc* phase. The in-plane (\parallel) loop of 57.3 at% Fe,Co in Fig. 3 is almost a straight line, confirming the single-phase nature of this sample. As the Fe,Co concentration increases, the soft phase appears and the in-plane loop expand into a shape with non-zero M_r and H_c . This is consistent with the two-phase

TABLE I. Magnetic properties of Fe-Co-Pt films. The Fe: Co atomic ratio is kept at 65: 35, and the thickness is 20 nm. The saturation magnetization M_s refers the value of 100% packing density, and $(BH)_{max}$ is the nominal energy product.

| Composition (at %) | | | M_s | H_c | $(BH)_{max}$ |
|--------------------|------|------|------------------------|-------|--------------|
| Fe | Co | Pt | (emu/cm ³) | (kOe) | (MGOe) |
| 37.2 | 20.1 | 42.7 | 1245 | 32 | 52.4 |
| 38.0 | 20.4 | 41.6 | 1289 | 26 | 59.7 |
| 38.7 | 20.8 | 40.4 | 1332 | 25.2 | 55.8 |
| 39.4 | 21.2 | 39.3 | 1355 | 13.7 | 60.3 |
| 40.2 | 21.6 | 38.2 | 1382 | 12.1 | 64.1 |
| 40.9 | 22.0 | 37.1 | 1416 | 8.9 | 58.4 |

nature deduced from the XRD pattern. A detailed discussion of the slope dM/dH of the in-plane loop was presented in Ref. 6.

It must be pointed out that Table I lists the best properties of the current films achievable. M_s was calculated based on the nominal film volume measured by deposition rate. M_s refers to the property of the material with 100% packing density. However, the TEM image in Fig. 2 shows that the film has gaps and the packing density is not 100%. Therefore the M_s of the film is smaller than those listed in Fig. 1. And the energy product $(BH)_{max}$ shown in Table I is the “nominal” energy product. The $(BH)_{max}$ value is correct for a single grain/particle observed in Fig. 2 which has 100% packing density. For the whole film of composition 61.8 at% Fe,Co, the measured packing density from TEM image is about 80%, and the maximum $(BH)_{max}$ of the film is 41 MGOe instead of 64 MGOe. In making bulk magnets, if the packing density is increased, the coercivity will be decreased as decoupling mechanism is weakened. The energy product $(BH)_{max}$ will be a maximum at the proper combination of M_s and H_c with optimum packing density. For example, assuming the coercivity can be maintained at a high enough value, the energy product of the best film would result in an energy product of 51.8 MGOe if the packing density were increased to 0.9.

V. CONCLUSIONS

A nearly perfect (001) alignment of the $L1_0$ structure (Fe,Co)Pt plus a *fcc* structure Fe(Co,Pt) can be epitaxially grown on the (001) MgO single crystal substrate at a temperature of 830°C by co-sputtering Fe, Co, and Pt targets. These films feature isolated magnetic grains of dimension about 100 nm. Excellent magnetic properties are obtained including high coercivities up to 32 kOe, high M_s up to 1416 emu/cm³, and high nominal granular energy product up to 64 MGOe. In order to achieve high energy products in granular exchange-coupled materials, it is necessary to increase the packing density while still maintaining sufficient coercivity. This may be achieved by separating the grains with a very thin (<1 nm) non-magnetic material to sustain sufficient inter-granular exchange decoupling.

ACKNOWLEDGMENTS

This work is supported by the U.S. Department of Energy, Office of Basic Energy Sciences, Division of Materials Sciences and Engineering under Award No. DE-FG02-04ER46152 and NCMN at the University of Nebraska, Lincoln.

¹E. F. Kneller and R. Hawig, *IEEE Trans. Magn.* **27**, 3588 (1991).

²R. Skomski and J. M. D. Coey, *Phys. Rev. B* **48**, 15812 (1993).

³D. J. Sellmyer, *Nature* **420**, 374 (2002)

⁴J. P. Liu, Y. Liu, and D. J. Sellmyer, *Appl. Phys. Lett.* **72**, 483 (1998).

⁵W. Liu, Y. Liu, R. Skomski, and D. J. Sellmyer, *Advanced Magnetic Materials I: Nanostructural Effects*, edited by Y. Liu, D. J. Sellmyer, and D. Shindo (Springer, Berlin, 2006), p. 182.

⁶J. Liu, T. A. George, R. Skomski, and D. J. Sellmyer, *Appl. Phys. Lett.* **99**, 172504 (2011).

⁷J. M. Maclaren, S. D. Willoughby, M. E. McHenry, B. Ramalingam, and S. G. Sankar, *IEEE Trans. Magn.* **37**, 1277 (2001).

⁸R. Skomski, J. P. Liu, and D. J. Sellmyer, *J. Appl. Phys.* **87**, 6334 (2000).